Impact of climate change on global malaria distribution

Cyril Caminade[a,b,1], Sari Kovats[c], Joacim Rocklov[d], Adrian M. Tompkins[e], Andrew P. Morse[b], Felipe J. Colón-González[e], Hans Stenlund[d], Pim Martens[f], and Simon J. Lloyd[c]

[a]Institute of Infection and Global Health, Department of Epidemiology and Population Health and [b]School of Environmental Sciences, Department of Geography and Planning, University of Liverpool, Liverpool L69 7ZT, United Kingdom; [c]Department of Social and Environmental Health Research, London School of Hygiene and Tropical Medicine, London WC1E 7HT, United Kingdom; [d]Department of Public Health and Clinical Medicine, Epidemiology and Global Health, Umea University, 901 87 Umea, Sweden; [e]Abdus Salam International Centre for Theoretical Physics, I-34151Trieste, Italy; and [f]Maastricht University, 6211 LK, Maastricht, The Netherlands

Edited by Hans Joachim Schellnhuber, Potsdam Institute for Climate Impact Research, Potsdam, Germany, and approved January 10, 2014 (received for review January 31, 2013)

Malaria is an important disease that has a global distribution and significant health burden. The spatial limits of its distribution and seasonal activity are sensitive to climate factors, as well as the local capacity to control the disease. Malaria is also one of the few health outcomes that has been modeled by more than one research group and can therefore facilitate the first model intercomparison for health impacts under a future with climate change. We used bias-corrected temperature and rainfall simulations from the Coupled Model Intercomparison Project Phase 5 climate models to compare the metrics of five statistical and dynamical malaria impact models for three future time periods (2030s, 2050s, and 2080s). We evaluated three malaria outcome metrics at global and regional levels: climate suitability, additional population at risk and additional person-months at risk across the model outputs. The malaria projections were based on five different global climate models, each run under four emission scenarios (Representative Concentration Pathways, RCPs) and a single population projection. We also investigated the modeling uncertainty associated with future projections of populations at risk for malaria owing to climate change. Our findings show an overall global net increase in climate suitability and a net increase in the population at risk, but with large uncertainties. The model outputs indicate a net increase in the annual person-months at risk when comparing from RCP2.6 to RCP8.5 from the 2050s to the 2080s. The malaria outcome metrics were highly sensitive to the choice of malaria impact model, especially over the epidemic fringes of the malaria distribution.

global climate impacts | disease modeling | uncertainty

Health priorities vary between countries and also change significantly over time. One of the factors that governments are concerned with preparing for over decadal timescales is the potential impact that environmental and climate change may have on health and welfare (1, 2). These impacts are complex and multifaceted and include the potential for changing climate to alter in both time and space the burden of vector-borne diseases, including malaria.

Malaria causes a significant burden of disease at the global and regional level (3). Malaria is a mosquito-borne infectious disease caused by parasitic protozoans of the genus *Plasmodium* (*vivax*, *malariae*, *ovale*, *knowlesi*, and *falciparum*) and is transmitted by female mosquito vectors of the *Anopheles* species. The spatial limits of the distribution and seasonal activity are sensitive to climate factors, as well as the local capacity to control the disease. In endemic areas where transmission occurs in regular long seasons, fatality rates are highest among children who have not yet developed immunity to the disease. In epidemic areas where malaria transmission occurs in short seasons or sporadically in the form of epidemics it is likely to cause severe fatalities in all age categories. Following the Global Malaria eradication program launched by the World Health Organization (WHO) in the 1950s, 79 countries eliminated malaria. Most of this progress was achieved in the extratropics (Eurasia, northern America, most of northern Africa, and Australia) where malaria transmission was highly seasonal owing to temperate climatic conditions and mainly caused by *P. vivax* (4). In the early 1970s WHO abandoned the idea of malaria elimination in the tropics, especially in Africa, owing to deficiencies in local public health services and the severity of *Plasmodium* infections in endemic areas, and replaced it by a control policy using modern control measures such as vector control through insecticide spraying, use of bed nets, systematic early detection and treatment of cases. Between 2000 and 2010 the incidence of malaria has fallen by 17% globally and by 33% in the African regions. There were 655,000 reported malaria deaths in 2010, of which 86% were of children under 5 y of age. In 2010, most of the malaria deaths occurred in Africa (91% of the global burden) and were due to *P. falciparum* (98% of infections), which causes the most severe clinical form of the disease (5).

Malaria is one of the few climate-sensitive health outcomes that has been modeled by more than one research group and can therefore facilitate a more thorough assessment of possible climate change effects using a multimodel intercomparison. Several global (6, 7) and regional assessments (8–10) have now been published using a range of malaria impact models and climate scenarios, but with varying results. Some divergence may be due to the malaria modeling approaches used in the earlier studies. Previous discussions of the relative merits of biological versus empirical statistical models have focused on the incomplete parameterization of the biological models (11). Conversely, statistical models are unable to completely separate out climate and nonclimate factors that determine the current distribution of malaria (6). To facilitate comparison of impacts under a range of climate scenarios and malaria models, a structure is needed that

Significance

This study is the first multimalaria model intercomparison exercise. This is carried out to estimate the impact of future climate change and population scenarios on malaria transmission at global scale and to provide recommendations for the future. Our results indicate that future climate might become more suitable for malaria transmission in the tropical highland regions. However, other important socioeconomic factors such as land use change, population growth and urbanization, migration changes, and economic development will have to be accounted for in further details for future risk assessments.

Author contributions: C.C., S.K., J.R., A.M.T., and A.P.M. designed research; C.C., A.M.T., and S.J.L. performed research; C.C., A.M.T., F.J.C.-G., H.S., and S.J.L. analyzed data; and C.C., S.K., J.R., A.M.T., and P.M. wrote the paper.

The authors declare no conflict of interest.

This article is a PNAS Direct Submission.

[1]To whom correspondence should be addressed. E-mail: Cyril.Caminade@liverpool.ac.uk.

This article contains supporting information online at www.pnas.org/lookup/suppl/doi:10.1073/pnas.1302089111/-/DCSupplemental.

differentiates variability originating from the different inputs and methods in the impact estimates.

There are limits to the usefulness of modeling changes in future malaria distribution owing to anthropogenic climate change (11) because important drivers of disease transmission are not yet included, such as population and vector movement, technological development, vector and disease control, urbanization, and land use change (12). Indeed, all future projections of malaria in a warmer world need to be put in the context of the observed global decline in the disease over the 20th century, mainly owing to human interventions (13).

Detailed mapping of current transmission is required for targeting control measures in the present (14). For climate impacts assessment, however, it is important to understand how the structure and parameterizations of the individual models account for any divergent results and to estimate the relative contribution of climate effects on malaria with respect to intervention and other nonclimate effects to assess confidence in future scenarios.

This project is part of the Inter-Sectoral Impact Model Intercomparison Project collaboration that aims to advance understanding of impact models by developing methods for intercomparison (15). Quantitative estimates of impacts and uncertainties have been produced for a range of socioeconomic outcomes, such as agriculture and water resources. The objective of the research was to produce a new set of health global impact assessments using five malaria models: LMM_RO (16), MIASMA (7), VECTRI (17), UMEA (6), and MARA (18) driven by climate outputs from five global climate models (GCMs) using the four Representative Concentration Pathways (RCPs) emissions scenarios developed for the fifth Intergovernmental Panel on Climate Change (IPCC) assessment report (19). The LMM_RO, MARA, and MIASMA models only allow the investigation of climatic suitability for malaria transmission, whereas the fully dynamical VECTRI model considers the impact of climate, surface hydrology, and population densities on malaria distribution. The UMEA model considers the impact of the gross domestic product per capita in combination with climate and population densities to model endemic malaria distribution. The first aim is to compare past distributions of malaria using the malaria models driven by observed climatic and socioeconomic data with "observed" malaria endemicity estimates (which include all potential climatic and socioeconomic effects on malaria distribution). Given the different designs and parameterizations of the malaria impact models (MIM) as they were originally developed for different regions and scientific objectives, they might significantly differ from the observed estimates. We then mapped future climate-based distributions of malaria and estimated populations at risk under the new emissions scenarios accounting for population growth and estimate the relative uncertainty and its evolution in time related to the global MIM, the climate model uncertainty inherit in the driving GCMs and the emission scenario uncertainty from the RCPs. An assessment of the different malaria models' sensitivity to climate change was then carried out before providing final conclusions (further details about individual MIM outcome can be found in *SI Appendix*).

Results

Fig. 1 shows observed and simulated malaria distribution for the 1900s and the 2000s at the global scale. Before intervention,

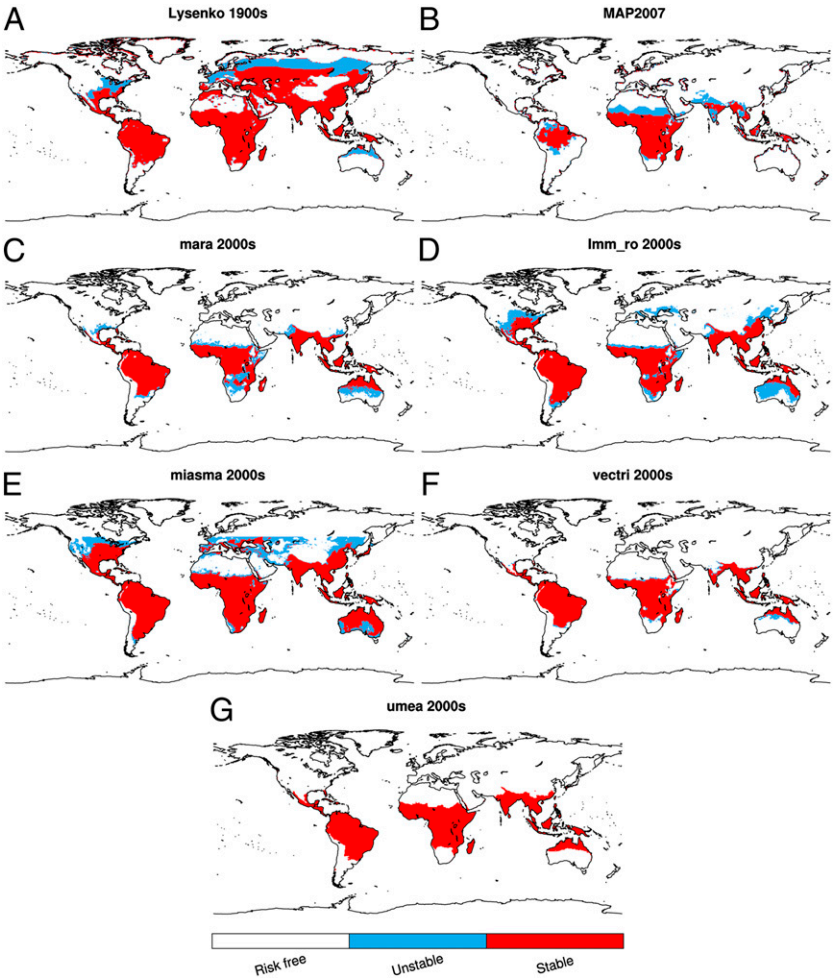

Fig. 1. Observed (*A* and *B*) and simulated malaria distribution (three categories: risk-free in white, unstable/epidemic in blue, and stable/endemic in red) for five malaria models (*C*, *D*, *E*, *F* and *G*). For the observation (*A* and *B*) all endemic subcategories (hypoendemic, mesoendemic, hyperendemic, and holoendemic) have been included in the stable category. The 1900s data (*A*) are based on ref. 38 (considers all plasmodium infections), and the 2000s data (*B*) are based on ref. 14 (considers only *P. falciparum* infections). For the simulations, unstable malaria is defined for a length of the transmission season (LTS) ranging between 1 and 3 mo, and suitable is defined for LTS above 3 mo (based on TRMMERAI control runs for the period 1999–2010; *SI Appendix*, Fig. S11 shows the CRUTS3.1 control runs). The TRMMERAI runs are constrained to span 50°N–50°S owing to the TRMM satellite data availability. For the UMEA malaria model only estimates of stable malaria were available.

malaria was highly epidemic in north-central Europe, over northern Russia, northern Australia, and in the northeastern United States; stable malaria transmission occurred in the Mississippi Valley (United States), central and south America, southern Africa, India, Malaysia–Indonesia, China, and over a large area covering the Middle East and south-central Russia (Fig. 1*A*). A similar contemporary map has been produced for the *P. falciparum* parasite (14). Its contemporary distribution is now mainly restricted to the tropics (Fig. 1*B*), and a large decrease in malaria endemicity has been observed worldwide, mainly owing to human intervention (13). Malaria has been eliminated in Europe, the United States, Russia, most of China, and Australia and has been significantly reduced in Central and South America and India and, to a lesser extent, over Africa (4).

Before intervention, the MIASMA model seems to provide the most realistic picture of malaria distribution with respect to observations at the global scale (Fig. 1 *E* vs. *A*). However, the simulated extension shown over Australia and North America seems relatively unrealistic, and this model does not capture the northward extension over Europe and Russia. This is not surprising, because all malaria models have been parameterized for *P. falciparum*, but the 1900s estimates includes all plasmodium species. Stable malaria transmission is consequently restricted to the tropics (Central and South America, Africa, India, Thailand, Malaysia, Indonesia, and northern Australia) for the MARA (Fig. 1*C*), LMM_R0 (Fig. 1*D*), VECTRI (Fig. 1*F*), and UMEA (Fig. 1*G*) models during the 2000s. The simulated malaria distribution patterns are generally consistent with the MAP2007 estimates (14) over the tropics (Fig. 1*B*) with, however, significant differences per model and per region. All malaria models simulate endemic malaria transmission over a large area covering northern Australia, but malaria has been eradicated in Australia. They also simulate endemic transmission over a large area in South America, but this is now restricted to the northern half of the South American continent. The MARA and VECTRI models provide the most realistic picture for *P. falciparum* distribution with respect to the MAP2007 analysis, but they generally tend to overestimate malaria endemicity over India, Central America, and southern Asia (Laos, Cambodia, Thailand, Burma, and southwestern China). The LMM_RO model simulates climate to be suitable for *P. falciparum* transmission in the Mississippi Valley (Fig. 1*D*), and this was observed in the 1900s before malaria was eradicated from the North American continent (Fig. 1*A*). The results from the malaria impact models driven by climate-only parameters need to be put in the context of an observed decline in malaria endemicity over the 20th century, mainly owing to intervention and related to other socioeconomic factors (*SI Appendix*, Fig. S1*A*). The agreement between observed and simulated malaria endemicity trends over the 20th century is restricted to a few regions of Africa (West Africa and a few regions over the African highlands) and South America (*SI Appendix*, Fig. S1 *B–D* vs. *A*). This does not obviously imply a direct causality between climate and malaria distribution trends but suggests that climate might have partly contributed to the overall trends over those regions. Generally, the historical experiments agree fairly well with the malaria control runs driven by climate observations (*SI Appendix*, Fig. S2), with a few differences that can be spotted over India for the HadGem2-ES and IPSLCM5A-LR experiments, only confirming the validity of the bias correction technique used with the global climate model data for present-day conditions.

The effect of future climate scenarios on the distribution of malaria for all five malaria models is summarized in Fig. 2. The maps show changes in the length of the malaria transmission season (LTS). Areas where the multimodel agreement is greater than 60% are hatched. The models show a consistent increase in the simulated LTS over the highlands at the regional scale. This can be seen over eastern Africa, South Africa, central Angola, the plateaux of Madagascar, Central America, southern Brazil, eastern Australia, and at the border between India and Nepal. Conversely, a consistent decrease is shown over tropical regions such as western Africa, the coasts of India, northern Australia, Malaysia, and South America. Fig. 3 shows the effect of climate scenarios on future populations at risk for malaria in Africa. The net effect of future climate change (for all emission scenarios) is relatively small, with large regional differences. Eastern Africa is the only region to show significant increases in the person-months at risk, but even here the range of results includes some projections of no net effect. A slight decrease in the population at risk is also shown over western Africa. However, the uncertainty of the malaria modeling method varies greatly in most regions (*SI Appendix*, Fig. S3). A more formal quantification of the future uncertainties was attempted using a linear decomposition of the variance, and this was displayed as a map for different time slices in the future (*SI Appendix*, Fig. S4). Generally, the largest uncertainties are associated with the methodology (e.g., the malaria models used). The uncertainties related to the driving GCMs are large over the northern fringe of the Sahel and

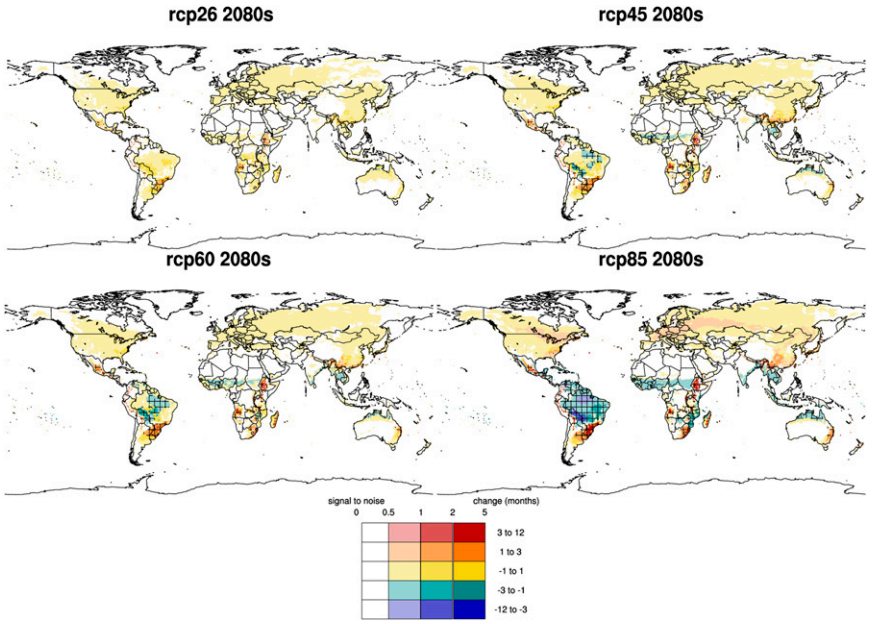

Fig. 2. The effect of climate scenarios on future malaria distribution: changes in LTS. Each map shows the results for a different emission scenario (RCP). The different hues represent change in LTS between 2069–2099 and 1980–2010 for the ensemble mean of the CMIP5 subensemble. The different saturations represent signal-to-noise ratio (μ/Sigma) across the super ensemble (the noise is defined as one SD within the multi-GCM and multimalaria ensemble). The hatched area shows the multimalaria multi-GCM agreement (60% of the models agree on the sign of changes if the simulated absolute changes are above 1 mo of malaria transmission).

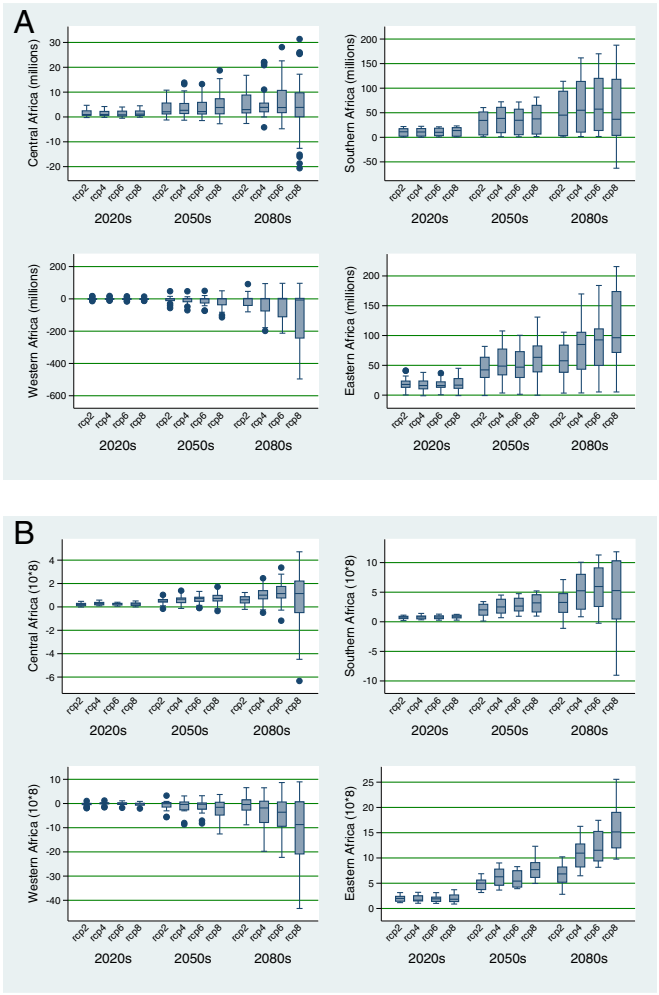

Fig. 3. The estimated population at risk owing to climate change impacts on malaria distribution for three time periods for four selected regions in Africa. (*A*) Additional population at risk for malaria owing to climate change based on the MARA, MIASMA, LMM, VECTRI, and UMEA models. (*B*) Additional person-months at risk for malaria based on the MARA, MIASMA, LMM, and VECTRI models.

over Brazil. This is consistent with the diverging rainfall projections shown by the various GCMs over those regions. The uncertainties related to the emission scenarios are relatively small, but they grow as a function of time (especially over South America and central Africa).

Given those uncertainties, the different malaria model sensitivities to climate change are further investigated for epidemic (*SI Appendix*, Fig. S5) and endemic transmission zones (*SI Appendix*, Figs. S6–S10). *SI Appendix*, Fig. S5 compares the future (2080s) and recent location of the simulated malaria epidemic belt based on the rcp85 scenario. The LMM_RO and MIASMA models tend to simulate a northward shift of the malaria epidemic belt over central-northern Europe, Russia, northern Asia, and northern America. This is unlikely to translate to increased malaria morbidity in reality provided that health surveillance systems in these regions maintain their capacity to identify and suppress primary imported infections efficiently. However, increasingly suitable climatic conditions might likely increase the incidence of autochthonous malaria cases in developed countries where competent malaria vectors are present, and those autochthonous cases generally have high fatality rates. Over the Sahel, the MIASMA and MARA model simulate a northward shift of the epidemic belt, whereas the most sophisticated dynamical models such as VECTRI and LMM_RO simulate a southward shift of the epidemic belt and a northward shift over southern Africa (consistent with ref. 10). As LTS decreases significantly over South America (Fig. 2) those models tend to simulate a shift from endemic to epidemic transmission over this region in the future climate. *SI Appendix*, Figs. S6–S10 describe changes in endemic malaria transmission for the different malaria models for the 2080s under the rcp85 emission scenario. All malaria models consistently simulate climate to become increasingly suitable for malaria transmission over the African highlands. Generally, the MIASMA malaria model tends to simulate an increase in climate suitability for endemic malaria transmission over central Europe and North America in the future. The UMEA model simulates endemic transmission over arid areas such as the northern edge of the Sahel and over the Middle East and central Australia (unrealistic changes given the aridity of those regions). MARA tends to simulate suitable future climate conditions for endemic transmission over the northern edge of the Sahel, southern Africa, western India, and southwestern China. The most sophisticated malaria models (LMM_RO and VECTRI) behave similarly; a large area over South America, northern Australia, the northern Sahel, southern Africa, India, Laos, Vietnam, Thailand, and Cambodia is simulated to become unsuitable for endemic malaria transmission in the future. However, those changes are sensitive to the driving GCMs, especially near the edges of the current malaria distribution.

Discussion

The results of this multimalaria model, multi-GCM, multiscenario intercomparison exercice are consistent with previous studies in indicating that the most significant climate change effects are confined to specific regions (highlands in Africa and parts of South America and southeastern Asia); in other regions climate change is likely to have no or a lesser effect on malaria owing to other important socioeconomic factors. Large uncertainties are present in the multimodel ensemble, especially over the epidemic fringes of the current malaria distribution. The impact of climate change on future malaria must be seen in the current context of a decline in malaria at global scale (13); however, there are concerns about future support for national-level malaria control efforts (4).

Climate-induced effects are more consistent with the observed changes over a few regions of Africa and South America. Climate change may have significant impacts in the east African highland region in the future, where the population at risk is large. This corroborates with the assessment "Human health, already compromised by a range of factors, could be further negatively impacted by climate change and climate variability, e.g., malaria in southern Africa and the East African highlands (high confidence)" that was published in the Fourth Assessment Report of the IPCC (20). Generally greater climate impacts across the multimodel ensemble are shown under the higher emission scenario (RCP8.5) for the end of the 21st century. There is no clear agreement between models at the lower rate of warming and for near-term projections.

This assessment has made an important advance in describing the uncertainty associated with future climate change impacts on global malaria distributions. Impacts on malaria transmission are considered an important consequence of future climate change, although it should be recognized that changes in malaria are unlikely to be a major contributor to modifications in the total burden of disease owing to global climate change (2). Projections of land use change, population growth, migration changes, and economic development were neglected in these models, all of which will alter the potential transmission bounds set by climate (13). The direct and indirect knock-on effects of climate change (on social, economic, political, and land use changes) and other nonclimatic disease driver changes will ultimately affect the changing vulnerability of the population and its ability to cope with and respond to disease burdens (21); this should be accounted for in a full assessment. In addition, the malaria parasite and its vector may adapt to evolving environmental conditions over

time, questioning the present approach of applying the present temperature-dependent life cycle rates (dynamical models) or climatic disease bounds (statistical models) to future climate conditions (22). As the biological models develop further in complexity to incorporate these effects, disparity between the impact models may widen rather than reduce, raising the issue of whether the simplest models should remain in future impact modeling ensembles. Further research on modeling malaria should also be undertaken at regional or national scales, with validated models, to identify more accurately those populations most at risk, based on regional environmental and socioeconomic changes (23). Many factors will determine the time at which individual countries achieve the capacity to control the disease. These will need to be addressed in future assessments of the potential impact of climate change on global malaria.

Materials and Methods

MIM Descriptions. All malaria models have been parameterized to simulate P. *falciparum* transmission. A common metric was used to intercompare all malaria models. The LTS of malaria was calculated for each MIM based on different assumptions (details are given in the following). To avoid spurious results from small changes in low transmission regions, a minimum of 4 mo of continuous transmission were required to indicate whether the climate was suitable for malaria in a given year. Thus, we defined climate suitability (CS) for malaria such as CS = 1 if LTS > 3 mo. Unstable transmission was defined for 1 < LTS ≤ 3. For UMEA, only estimates of stable transmission were available.

LMM_RO monthly model (model 1). The model used here is a simplified version of the vector transmission potential model formulated by Jones (16) and uses monthly rainfall and temperature data as inputs. The number of emerging adult mosquitoes at the beginning of each month is taken to be proportional to the rain falling during the previous month. The mosquito population is then combined with the biting rate, sporogonic cycle length, and survival probability calculated from monthly temperatures, together with the other parameters provided as input to the model, to derive the reproduction ratio, R_0. If $R_0 > 1$ then malaria transmission occurs for a given month. The derivation of R_0 is based on the transmission model component of the full LMM (Liverpool Malaria Model), which is a weather-driven, mathematical–biological model of malaria that was originally formulated by Hoshen and Morse (24) and has been applied at national and regional scales. The full LMM model uses daily rainfall and temperature data as inputs. It has been successfully validated against a 20-y clinical record for Botswana (25). For LMM_RO, LTS = 1 for a given month if Ro > 1.

MARA model (model 2). The MARA seasonality model was original derived to map start and end months of the malaria transmission season for locations in Africa based on monthly long-term averages of rainfall and temperature (18). It was modified (16) to create a simple model of seasonal malaria transmission. The basic requirements of the model are 3 mo of rainfall at a minimum value (60 mm) together with a catalyst month specified by another minimum rainfall value (80 mm). Temperature is constrained to be greater than a threshold value (19.5 °C) plus a seasonality index calculated from the SD of the monthly rainfall. The resulting output is either "on," indicating the malaria season is in progress, or "off," indicating one or more of the conditions have not been met. For MARA, LTS is a direct output of the model.

VECTRI model (model 3). VECTRI is a mathematical model for malaria transmission that accounts for the impact of temperature and rainfall variability on the development cycles of the malaria vector in its larval and adult stage, and also of the parasite itself. The parameterizations for the biological processes are taken from the literature for the *Anopheles gambiae* vector and the *P. falciparum* species of the parasite. Temperature affects the sporogonic and gonotrophic cycle development rates according to the standard degree-day model, and higher temperature increases the mortality rates for adult vectors (18). Rainfall effects on transmission are represented by a simple, physically based model of surface pool hydrology, whereby rainfall increases available breeding sites that subsequently decay through evaporation and infiltration, and intense rain events decrease early-stage larvae through flushing (26). In reality, land surface properties also modify the availability of breeding sites, but VECTRI does not presently model these. VECTRI accounts for human population density in the calculation of biting rates. Higher population densities lead to a dilution effect, resulting in lower parasite ratios (PRs) in urban and peri-urban environments compared with nearby rural locations. In this respect the model is able to reproduce the reduction in entomological inoculation rates (EIR) and PR with increasing population density that has been widely observed in African field studies (27). Although the VECTRI model could include the impact of future population growth and urbanization on transmission intensity, these factors were inhibited in this study to ensure the experiment assumptions are equal for all models. The model is designed for regional to continental scales at high spatial resolutions of up to 5–10 km. VECTRI is the only full dynamical model participating in the study operating on a daily time step and accounting for subseasonal variations in climate. As a consequence the VECTRI model is the only one that requires a representation of human migration to transport malaria parasites to new regions that may become suitable for future transmission. Migration was estimated by mixing population with a coefficient equivalent to 1% population exchange per year. For full details of the models mathematical framework and its evaluation see ref. 17. For VECTRI, LTS = 1 for a given month if EIR > 0.01 d^{-1}.

UMEA statistical model (model 4). The malaria model is a spatial empirical-statistical model created at the Umea University (6). The malaria model uses climate and socioeconomic factors to determine the spatial distribution of endemic malaria (*P. falciparum*) transmission. Generalized additive logistic regression models were used to empirically estimate the relationship between endemic malaria transmission and climatic factors on a global scale using the output of the Malaria Atlas Project Bayesian statistical model, which combines malaria survey data with environmental and climate predictors to provide a gridded malaria analysis for 2010 (28). Flexible nonlinear relationship and interaction between climate factors on the probability of malaria transmission were initially established and compared with simpler models to find a simple model with good fit. For UMEA, only binary CS estimates were available.

MIASMA model (model 5). The malaria module of the MIASMA model incorporates temperature effects on the survival probability and biting frequency of mosquitoes (7). The various temperature-dependent relationships are aggregated into the entomological version of the equation for R_0. Owing to the lack of data on several key parameters, these are set as biologically plausible constants, allowing the calculation of the critical vector density required for sustainable disease transmission (e.g., $R_0 > 1$). This threshold is lower under more suitable climate conditions. The inverse of the critical density threshold, the 'transmission potential' (TP), is used as a relative measure of transmission intensity under different climatic conditions. The model assumes that a minimum level of monthly rainfall of 80 mm is essential for malaria transmission, based on the value used in the MARA project (18, 29). In this assessment, the modeled distribution is not constrained by the current distribution of malaria vectors (7). For MIASMA, LTS = 1 for a given month if TP > 0.

Climate and Population Scenario Data. The Coupled Model Intercomparison Project Phase 5 (CMIP5) project is collaboration among climate modelers to produce a consistent set of climate model outputs for the RCP emissions scenarios. The CMIP experimental design is described in ref. 30. The CMIP5 output was bias-corrected by the Potsdam Institute for Climate Impact Research (31) for this project to ensure statistical agreement with the observed Watch Forcing Data dataset over the period 1960–1999. All climate scenarios were mapped to a uniform half-degree grid. The RCP emission scenarios (RCP2.6, RCP4.5, RCP6, and RCP8) represent a range of climate forcings. Climate scenarios were available for all RCPs and for five global climate models: HadGem2-ES, IPSL-CM5A-LR, MIROC-ESM-CHEM, GFDL-ESM2M, and NorESM1-M. The five models were selected to give a wide range of temperature and rainfall changes, rather than a representation of the likelihood of future climate change (15). Climate data were available to 2100; however, malaria integrations were undertaken for three time slices (30-y averages): 2020s (2005–2035), 2050s (2035–2065), and 2080s (2069–2099), with the exception of VECTRI, which instead conducted century-long integrations from the present to 2100 using daily climate data.

To evaluate the respective bias-corrected baseline integrations, additional malaria integrations were conducted using two sets of gridded observed climate datasets. The first set used temperature and precipitation from the Climatic Research Unit (CRU) dataset v3.1 (32) for a period very close to the historical integrations 1980–2009. Because the CRU data were only available at monthly timescale, the VECTRI model was excluded from this analysis. The second set of integrations used the Tropical Rainfall Measuring Mission (TRMM) 3B42 dataset (33) with precipitation retrievals based on microwave and precipitation radar observations, supplemented with infrared information when the former was unavailable. The temperature information was derived from the interim reanalysis of the European Centre for Medium-Range Weather Forecasts (34). Both observed climate datasets (CRUTS3.1 and TRMMERAI) were aggregated to the half-degree grid of the CMIP5 climate data. Malaria integrations were also conducted for the modeled baseline period (historical) for each GCM (1980–2010).

For the assessment of future populations at risk for malaria we used a single population projection from the new Shared Socio-economic Pathway (SSP) set of socio-economic scenarios (35). We used the SSP2 population scenario, which projects a population of 9.5 billion people in 2055 (36). The national projections for 193 countries were converted to a gridded population product by first deriving a population map for 2000 scaling the gridded Gridded Population of the World v3 dataset (37) to match the national totals. This distribution was then projected into the future using national average projections to scale each grid point. A small number of countries not present in the dataset were assigned the global-mean population growth rate over the next century. The reference years for the population data were as follows: current climate, 2000; 2020s, 2020; 2050s, 2050; and 2080s, 2085 population.

Estimating Populations at Risk for Malaria. We estimated two population outcomes. The population at risk for malaria (PAR) was defined as the population present in an area where the climate was suitable for malaria transmission (averaged CS > 0.5). Person months at risk (PMAR) were calculated as the length of the transmission season multiplied by the population living in the grid cell. The climate change attributable PAR and PMAR were estimated as the difference between future population at risk for a given scenario compared with the population at risk under the current modeled climate. It was not possible to estimate PMAR for the UMEA model, which only produces annually averaged CS binary outputs. All estimates were aggregated to world regions (15).

Model Validation. To attempt some validation of the different malaria models, we compared the output of the malaria models for the two observed climate baseline datasets and GCM modeled baselines and compared those outputs with other published malaria endemicity maps based on ref. 13. Preintervention malaria endemicity estimates are based on a major synthesis of historical records, documents, and maps of a variety of malariometric indices for the four major *Plasmodium* species (*malariae, ovalae, vivax*, and *falciparum*) that was conducted by Lysenko (38). Recent malaria endemicity estimates (*P. falciparum*) have been derived from the Malaria Atlas Project (MAP) for comparison purposes (14). The MAP dataset is an analysis integrating survey data with environmental and socioeconomic predictors in a Bayesian model to produce a "best guess" of mapped malaria endemicity at global scale. These datasets were digitized from the original papers. This allows a comparison with the malaria model outputs for which the epidemic and stable transmission regions are defined for a criterion based on LTS.

Supplementary Information. Further details about the MIM validation, the estimation of the uncertainties in the super ensemble, and changes in endemic and epidemic transmission for each MIM are provided in *SI Appendix*.

ACKNOWLEDGMENTS. The Inter-Sectoral Impact Model Intercomparison Project Fast Track project was funded by the German Federal Ministry of Education and Research with project funding reference number 01LS1201. A.P.M., C.C., and F.J.C.-G. were jointly funded by the European Union FP7 Quantifying Weather and Climate Impacts on Health in Developing Countries (QWeCI) and HEALTHY FUTURES projects. C.C. and A.P.M. also acknowledge funding support from the End-to-End Quantification of Uncertainty for Impacts Prediction (EQUIP) Natural Environmental Research Council Project NE/H003487/1.

1. Costello A, et al. (2009) Managing the health effects of climate change. *Lancet* 373(9676):1693–1733.
2. McMichael AJ, et al. (2004) Climate change. *Comparative Quantification of Health Risks: Global and Regional Burden of Disease Due to Selected Major Risk Factors*, eds Ezzati M, et al. (World Health Organization, Geneva), Vol 2, pp 1543–1649.
3. Murray CJ, et al. (2012) Global malaria mortality between 1980 and 2010: A systematic analysis. *Lancet* 379(9814):413–431.
4. Feachem RG, et al. (2010) Shrinking the malaria map: Progress and prospects. *Lancet* 376(9752):1566–1578.
5. WHO (2011) *World Malaria Report 2011* (World Health Organization, Geneva), pp 1–248.
6. Beguin A, et al. (2011) The opposing effects of climate change and socio-economic development on the global distribution of malaria. *Glob Environ Change* 21(4):1209–1214.
7. van Lieshout M, et al. (2004) Climate change and malaria: Analysis of the SRES climate and socio-economic scenarios. *Glob Environ Change* 14(1):87–99.
8. Snow RW, Hay S, Marsh K (2006) Report T5.8: Malaria in Africa: Sources, risks, drivers and disease burden 2005–2030. *Infectious Diseases*: *Preparing for the Future* (Office of Science and Innovation, London).
9. Tanser FC, Sharp B, le Sueur D (2003) Potential effect of climate change on malaria transmission in Africa. *Lancet* 362(9398):1792–1798.
10. Ermert V, Fink AH, Morse AP, Paeth H (2012) The impact of regional climate change on malaria risk due to greenhouse forcing and land-use changes in tropical Africa. *Environ Health Perspect* 120(1):77–84.
11. Rogers DJ, Randolph SE (2000) The global spread of malaria in a future, warmer world. *Science* 289(5485):1763–1766.
12. Tatem AJ, Guerra CA, Kabaria CW, Noor AM, Hay SI (2008) Human population, urban settlement patterns and their impact on Plasmodium falciparum malaria endemicity. *Malar J* 7:218.
13. Gething PW, et al. (2010) Climate change and the global malaria recession. *Nature* 465(7296):342–345.
14. Hay SI, et al. (2009) A world malaria map: Plasmodium falciparum endemicity in 2007. *PLoS Med* 6(3):e1000048.
15. Warszawski L, et al. (2014) The Inter-Sectoral Impact Model Intercomparison Project (ISI-MIP): Project framework. *Proc Natl Acad Sci USA* 111:3228–3232.
16. Jones A (2007) Seasonal ensemble prediction of malaria in Africa. PhD thesis (Univ of Liverpool, Liverpool).
17. Tompkins AM, Ermert V (2013) A regional-scale, high resolution dynamical malaria model that accounts for population density, climate and surface hydrology. *Malar J* 12:65.
18. Craig MH, Snow RW, le Sueur D (1999) A climate-based distribution model of malaria transmission in sub-Saharan Africa. *Parasitol Today* 15(3):105–111.
19. Moss RH, et al. (2010) The next generation of scenarios for climate change research and assessment. *Nature* 463(7282):747–756.
20. Confalonieri U, et al. (2007) Human health. *Climate Change 2007: Impacts, Adaptation and Vulnerability. Contribution of Working Group II to the Fourth Assessment Report of the Intergovernmental Panel on Climate Change*, eds Parry ML, et al. (Cambridge Univ Press, Cambridge, UK), pp 391–431.
21. McMichael AJ, Woodruff RE, Hales S (2006) Climate change and human health: present and future risks. *Lancet* 367(9513):859–869.
22. Hoffmann AA, Sgrò CM (2011) Climate change and evolutionary adaptation. *Nature* 470(7335):479–485.
23. Bouma MJ, Baeza A, terVeen A, Pascual M (2011) Global malaria maps and climate change: A focus on East African highlands. *Trends Parasitol* 27(10):421–422.
24. Hoshen MB, Morse AP (2004) A weather-driven model of malaria transmission. *Malar J* 3:32.
25. Jones A, Morse AP (2010) Application and validation of a seasonal ensemble prediction system using a dynamic malaria model. *J Clim* 23:4202–4215.
26. Paaijmans KP, Wandago MO, Githeko AK, Takken W (2007) Unexpected high losses of Anopheles gambiae larvae due to rainfall. *PLoS ONE* 2(11):e1146.
27. Kelly-Hope LA, McKenzie FE (2009) The multiplicity of malaria transmission: a review of entomological inoculation rate measurements and methods across sub-Saharan Africa. *Malar J* 8(1):19.
28. Gething PW, et al. (2011) A new world malaria map: Plasmodium falciparum endemicity in 2010. *Malar J* 10:378.
29. MARA/ARMA Collaboration (1998) Towards an atlas of malaria risk in Africa. First Technical Report of the MARA/ARMA Collaboration (MARA/ARMA, Durban, South Africa).
30. Taylor KE, Stouffer RJ, Meehl GA (2012) An overview of CMIP5 and the experiment design. *Bull Am Meteorol Soc* 93:485–498.
31. Hempel S, et al. (2013) A trend-preserving bias correction – the ISI-MIP approach. *Earth System Dynamics* 4:49–92.
32. Mitchell TD, Jones PD (2005) An improved method of constructing a database of monthly climate observations and associated high-resolution grids. *Int J Climatol* 25:693–712.
33. Huffman GJ, et al. (2007) The TRMM Multisatellite Precipitation Analysis (TMPA): Quasi-global, multiyear, combined-sensor precipitation estimates at fine scales. *J Hydrometeorol* 8:38–55.
34. Dee DP, et al. (2011) The ERA-Interim reanalysis: Configuration and performance of the data assimilation system. *Q J R Meteorol Soc* 137:553–597.
35. Van Vuuren DP, et al. (2012) A proposal for a new scenario framework to support research and assessment in different climate research communities. *Glob Environ Change* 22(1):21–35.
36. SSP Database (2012) Shared Socioeconomic Pathways database. Available at https://secure.iiasa.ac.at/web-apps/ene/SspDb.
37. Center for International Earth Science Information Network (2005) Gridded Population of the World, Version 3 (GPWv3) Data Collection (Columbia Univ, Palisades, NY).
38. Lysenko AJSI (1968)*Geography of Malaria: A Medico-Geographic Profile of an Ancient Disease*, ed Lebedew AW (Academy of Sciences, Moscow), pp 25–146.